



Published in final edited form as:

Biochemistry. 2009 September 1; 48(34): 8271–8278. doi:10.1021/bi900777s.

Interaction of Human DNA Polymerase α and DNA Polymerase I from *Bacillus stearothermophilus* with Hypoxanthine and 8-Oxoguanine Nucleotides [†]

Jennifer N. Patro, Milan Urban, and Robert D. Kuchta ^{*}

Department of Chemistry and Biochemistry, University of Colorado, UCB 215, Boulder, CO 80309

Abstract

To better understand how DNA polymerases interact with mutagenic bases, we examined how human DNA polymerase α (pol α), a B family enzyme, and DNA polymerase from *Bacillus stearothermophilus* (BF), an A family enzyme, generate adenine:hypoxanthine and adenine:8-oxo-7,8-dihydroguanine (8-oxoG) base pairs. Pol α strongly discriminated against polymerizing dATP opposite 8-oxoG, and removing N1, N⁶, or N7 further inhibited incorporation, whereas removing N3 from dATP dramatically increased incorporation (32-fold). Eliminating N⁶ from 3-deaza-dATP now greatly reduced incorporation, suggesting that incorporation of dATP (analogues) opposite 8-oxoguanine proceeds via a Hoogsteen base-pair and that pol α uses N3 of a purine dNTP to block this incorporation. Pol α also polymerized 8-oxo-dGTP across from a templating A, and removing N⁶ from the template adenine inhibited incorporation of 8-oxoG. The effects of N1, N⁶, and N7 demonstrated a strong interdependence during formation of adenine:hypoxanthine base-pairs by pol α and N3 of dATP again helps prevent polymerization opposite a templating hypoxanthine. BF very efficiently polymerized 8-oxo-dGTP opposite adenine, and N1 and N7 of adenine appear to play important roles. BF incorporates dATP opposite 8-oxoG less efficiently, and modifying N1, N⁶, or N7 greatly inhibits incorporation. N⁶, and to a lesser extent N1, help drive hypoxanthine:adenine base pair formation by BF. The mechanistic implications of these results showing that different polymerases interact very differently with base lesions are discussed.

Keywords

Fidelity; misincorporation; kinetics; mechanism; base-pair; Hoogsteen

Introduction

Accurate DNA replication is crucial for cell survival and in the case of multicellular organisms, important for preventing oncogenesis and subsequent death of the organism. Therefore, DNA polymerases should replicate DNA with as few errors as possible. Typical error rates are 10^{-3} – 10^{-6} per nucleotide replicated, indicating that these enzymes form correct base pairs much more efficiently than incorrect base pairs (1). In addition, some of these enzymes contain a 3'–5' exonuclease designed to remove misincorporated nucleotides.

How DNA polymerases choose whether or not to incorporate a nucleotide remains unclear. Even though structural, kinetic, and substrate mutagenesis studies have been variously

[†]This work was supported by grants from the NIH GM54194.

^{*}To whom correspondence should be addressed. kuchta@colorado.edu, Phone: 303-492-7027, FAX: 303-492-5894.

employed with different polymerases, the mechanism(s) that differentiate an efficiently polymerized base-pair from a poorly polymerized base-pair remain unclear and controversial. Multiple models exist, including base-pair shape, formation of Watson-Crick hydrogen bonds, and positive/negative selectors (2–5). Previous studies examining DNA polymerase α (pol α ¹), a B family polymerase, indicate that it uses a combination of negative selectivity to prevent misincorporation and positive selectivity (Watson-Crick hydrogen bond formation) to enhance correct dNTP polymerization, while shape does not play a significant role during incorporation (6). Different studies with Klenow Fragment, an A family polymerase, have given inconsistent results. Some studies have concluded that the shape of the incipient base pair plays a key role in fidelity, while others indicate that shape has no significant role (7–9).

In addition to the natural bases, polymerases will also confront modified bases generated by unwanted chemical reactions. Guanine is the most readily oxidized natural base (10), and the oxidized product, 8-oxoG, is an extremely important problem both when found in the DNA template and as a dNTP (11,12). 8-OxoG can flip into the *syn* conformation and then form base pairs with A (Figure 1), causing the common G:C to T:A mutation (13,14). Generating 8-oxoG lesions in *E. coli* greatly increased both G→T transversions due to polymerization of dATP opposite 8-oxoG and A→C transversions due to polymerization of 8-oxo-dGTP opposite A (15,16). Previous studies with *E. coli* have clearly demonstrated that significant concentrations of 8-oxo-dGTP can accumulate (17). To help solve this problem multiple repair pathways have evolved to recognize and remove 8-oxoG both from DNA strands and the nucleoside triphosphate pools (11,18,19).

Previous work showed that pol α incorporates dATP 7-fold more efficiently than dCTP opposite an 8-oxoG template lesion (20). No data exist on polymerization of 8-oxo-dGTP opposite of natural templates by pol α . In addition, no structural studies with respect to this lesion have been completed with pol α . However, the lesion has been examined structurally with RB69, a closely related B-family polymerase (21,22). The 8-oxoG:C base pair binds to RB69 similar to a normal base pair while the 8-oxoG:A base pair binds in the *syn* conformation (Figure 1) (23,24). In addition, it has been shown that other polymerases, such as Dpo4, will form 8-oxoG (*anti*):A (*syn*) base pairs (Figure 1), therefore this type of Hoogsteen base pair must be considered.

The Klenow fragment of *E. coli* DNA polymerase I, an A family polymerase, preferentially incorporates dCTP opposite a templating 8-oxoG (5) as well as 8-oxo-dGTP opposite a templating C (4). In contrast, another A family enzyme, DNA polymerase I from *Bacillus stearothermophilus* (BF) incorporates dATP 9-fold more efficiently than dCTP opposite 8-oxoG in the template (25). BF has also been extensively characterized structurally as the BF-DNA binary complex, both with normal DNA and DNA containing 8-oxoG lesions (25,26). When base-paired with C, 8-oxoG resides in the *anti* configuration, although a steric clash between O⁸ and the 4'-O causes substantial distortion of the backbone. In an A:8-oxoG base pair, however, the 8-oxoG exists as the *syn* conformer and the backbone appears normal.

A second base lesion, the conversion of guanine into hypoxanthine via deamination of N², also increases generation of A:I base pairs by both BF and pol α (27,28). This occurs both during

¹Abbreviations used: 1-Deaza-2'-deoxyadenosine triphosphate, 1-deaza dATP, 1DdATP; 3-Deaza-2'-deoxyadenosine triphosphate, 3-deaza dATP, 3DdATP; 7-Deaza-2'-deoxyadenosine triphosphate, 7-deaza dATP, 7DdATP; 3-Deaza-2'-deoxyguanosine triphosphate, 3-deaza dGTP, 3DdGTP; 3-Deazapurine-2'-deoxyriboside triphosphate, 3-deazapurine dNTP, 3DdPPT; 7-Deazapurine-2'-deoxyriboside triphosphate, 7-deazapurine dNTP, 7DdPPT; 1- β -D-2'-Deoxyribofuranosyl-(6-trifluoromethylbenzimidazole)-5'-triphosphate, 6CF3dBTP; 1- β -D-2'-deoxyribofuranosyl-(6-nitrobenzimidazole)-5'-triphosphate, 6NO₂dBTP; DNA polymerase α , pol α ; DNA polymerase I from *Bacillus stearothermophilus*, BF; Hypoxanthine, I; 8-Oxo-7,8-dihydroguanine, 8-oxoguanine, 8-oxoG; Purine-2'-deoxyriboside triphosphate, purine dNTP, dPPT; Tris-HCl, Tris(hydroxymethyl)aminomethane.

polymerization of dITP opposite A and dATP polymerization opposite hypoxanthine. In both cases, however, the two polymerases still showed a preference for generating C: hypoxanthine base pairs.

We have used a series of adenine analogues modified at N1, N3, N⁶, and N7 to better understand both how these enzymes polymerize 8-oxo-dGTP and dITP opposite A as well as dATP opposite 8-oxoG and hypoxanthine. Both during incorporation of the analogue dNTPs opposite A and dATP opposite the analogues, polymerization is more complicated than simple formation of Hoogsteen base pairs.

Experimental Procedures

Materials

All reagents were of the highest quality commercially available. Unlabeled natural dNTPs were from Sigma and radiolabeled dNTPs were from Perkin Elmer. dITP, 7-deaza-dATP, and 8-oxo-dGTP were from Trilink. 1-Deaza dATP and purine dNTP were prepared as previously described (6). Protected phosphoramidites of nucleosides containing the bases purine, 7-deaza-dA and hypoxanthine were from Glen Research. Synthetic DNA oligonucleotides were purchased from IDT or Biosearch. The two subunit p180-p70 polymerase complex was expressed in baculovirus-infected SF9 cells at the Tissue Culture Core Facility of the University of Colorado Health Sciences Center and purified as previously described (27,29,30). BF was a generous gift of Loreena Beese (Duke University).

Methods

5'-End Labeling of Primers and Annealing of Primer/Templates—DNA primers were 5'-[³²P]-labeled using polynucleotide kinase (New England Biolabs) and [γ -³²P]ATP (Perkin Elmer). The labeled primer was gel purified and annealed to the template as previously described (31,32).

Synthesis of nucleotide analogues—7-Deazapurine 6-Chloropurine (1.0 g, 6.6 mmol) was dissolved in a mixture of *i*PrOH (50 mL), water (20 mL) and triethylamine (5 mL). Palladium on charcoal (0.5 g, 10 %) was added and the flask was evacuated and filled with H₂ at standard pressure. The mixture was vigorously stirred while H₂ was continuously replaced. Palladium on charcoal was filtered off and the solvents were evaporated in vacuo to yield 0.74 g (95 %) of pure 7-deazapurine. ¹H NMR (400 MHz, CD₃OD): 8.97 (s, 1H, H-2), 8.73 (s, 1H, H-6), 7.51 (d, 1H, *J* = 2.8 Hz, H-8), 6.67 (dd, 1H, *J*₁ = 2.8 Hz, H-7).

9-β-D-(7-Deazapurin)-1',2'-deoxy-3',5'-di-*O*-(4-toluoyl)-D-ribofuranose. 7-Deazapurine (500 mg, 4.2 mmol) was dissolved in MeCN (100 mL) and NaH (5.9 mmol, 60 % in oil, 1.4 eq.) was added. The mixture was stirred 3 h at r.t. and then 1-chloro-3,5-bis(p-toluoyl)-2-deoxy-β-D-ribofuranose (1.9 g, 5 mmol) was added. The resulting dark brown slurry was stirred overnight, resulting in most of the slurry dissolving. The mixture was then poured into saturated aqueous NH₄Cl, extracted with EtOAc, and the product purified by chromatography on silica gel (100 mL) using a gradient from 50 % EtOAc/hexanes to EtOAc. The yield of colorless oil was 790 mg (41 %). ¹H NMR (400 MHz, CDCl₃): 8.94 (s, 1H, H-2), 8.87 (s, 1H, H-6), 7.98 (bdd, 2H, *J*₁ = 6.5 Hz, *J*₂ = 1.7 Hz, Tol), 7.94 (bdd, 2H, *J*₁ = 6.5 Hz, *J*₂ = 1.7 Hz, Tol), 7.40 (d, *J* = 3.8 Hz, H-8), 7.20–7.30 (m, 4H, 4xH-Tol), 6.89 (dd, 1H, *J*₁ = 8.7 Hz, *J*₂ = 5.7 Hz, H-1'), 6.56 (d, 1H, *J* = 3.7 Hz, H-7), 5.76 (dt, 1H, *J*₁ = 6.3 Hz, *J*₂ = 2.1 Hz, H-3'), 4.58–4.75 (m, 3H, H-5'a, H-5'b, H-4'), 2.91 (ddd, 1H, *J*_{gem} = 14.2 Hz, *J*₂ = 8.7 Hz, *J*₃ = 6.3 Hz, H-2'a), 2.84 (ddd, 1H, *J*_{gem} = 14.2 Hz, *J*_{2'b,1'} = 7.8 Hz, *J*_{2'b,3'} = 2.0 Hz, H-2'b), 2.43 (s, 3H, CH₃-Tol), 2.41 (s, 3H, CH₃-Tol).

9-β-D-(7-Deazapurine)-2'-deoxyribofuranose. 9-β-D-(1-Deazapurin)-2'-deoxy-3',5'-di-O-(4-toluoyl)-D-ribofuranose (0.68 g, 1.49 mmol) was deprotected in 30 min using 0.1 M MeONa in MeOH and purified by silica gel chromatography (20 mL) using a gradient of 0–20 % MeOH in CHCl₃. This procedure gave 0.27 g (82 %) of product. ¹H NMR (400 MHz, CD₃OD): 8.92 (s, 1H, H-2), 8.79 (s, 1H, H-6), 7.77 (d, 1H, *J*₁ = 3.7 Hz, H-8), 6.72 (dd, 1H, *J*₁ = 7.8 Hz, *J*₂ = 6.2 Hz, H-1'), 6.68 (d, 1H, *J* = 3.8 Hz, H-7), 4.92 (bs, 3H, OH, H₂O), 4.55 (m, 1H, H-3'), 4.02 (dd, 1H, *J*₁ = 6.7 Hz, *J*₂ = 3.7 Hz, H-4'), 3.80 (dd, 1H, *J*_{5'a, 5'b} = 12.0 Hz, *J*_{5'a, 4'} = 3.6 Hz, H-5'a), 3.73 (dd, 1H, *J*_{5'b, 5'a} = 12.0 Hz, *J*_{5'a, 3'} = 4.0 Hz, H-5'a), 2.68 (ddd, 1H, *J*_{gem} = 13.7, Hz, *J*₂ = 7.9 Hz, *J*₃ = 6.0 Hz, H-2'a), 2.43 (ddd, 1H, *J*_{gem} = 13.4 Hz, *J*_{2'b, 1'} = 6.0 Hz, *J*_{2'b, 3'} = 2.8 Hz, H-2'b).

9-β-D-(7-Deazapurine)-2'-deoxyribofuranose triphosphate. Nucleoside (0.2 mmol) was dissolved in dry Me₃PO₄ (0.5 mL) and the solution was cooled to 0 °C. POCl₃ (20 μL, 1.1 eq.) in Me₃PO₄ (0.3 mL) was drop wise added and the mixture was stirred for 2 h. A solution of triethylammonium pyrophosphate (5 eq. in DMF, 1 mL) was added followed by 1 drop of tributyl amine. The mixture was stirred another 3 h while warming to r.t. Crude product was poured into the solution of triethylammonium bicarbonate (50 mL, 0.01 M), water was evaporated and triphosphate, redissolved in water (200 mL) was purified by ion exchange chromatography on Sephadex-DEAE A-25 (Aldrich). The column was equilibrated with TEAB, the sample loaded and then eluted with a 0 to 1 M TEAB gradient. The triphosphate was identified by MALDI MS (negative M - 1 ion) with THAP as the matrix. Collected fractions were evaporated and purified by HPLC using a gradient of 0 to 50 % MeCN in 20 mM TEAA, pH 7.0 (triethylammonium acetate) giving a yield of 11 %. MS (MALDI, neg.): 474 (M - 1). ³¹P NMR (400 MHz, D₂O): - 8.64 (d, 1P, *J* = 48.8 Hz, α-P), - 10.35 (d, 1P, *J* = 49.6 Hz, γ-P), -22.14 (t, 1P, *J* = 48.8 Hz, β-P).

5'-(4,4-Dimethoxytrityl)-9-β-D-(7-deazapurine)-2'-deoxyribofuranose. 9-β-D-(7-Deazapurine)-2'-deoxyribofuranose (81 mg, 0.4 mmol) was dissolved in pyridine (2 mL), while triethylamine (70 μL), DMAP (catalytic amount) and dimethoxytritylchloride (140 mg, 2.6 mmol) were added. After the reaction was completed (24 h, analyzed by silica TLC in EtOAc), the mixture was poured into saturated NaHCO₃ and the product was extracted into EtOAc. Organic layers were washed with several portions of 1 % NaHCO₃, dried over MgSO₄ and solvents were evaporated under reduced pressure. The product was purified by silica gel chromatography (0–10 % MeOH in EtOAc). The reaction yielded 158 mg (82 %) of 5'-(4,4-dimethoxytrityl)-9-β-D-(7-deazapurine)-2'-deoxyribofuranose. ¹H NMR (400 MHz, CDCl₃): 8.90 (s, 1H, H-2), 8.81 (s, 1H, H-6), 7.11 – 7.44 (m, 10H, 1×H-8, 9×H-DMTr), 6.85 (t, 1H, *J*_{1', 2'} = 6.5 Hz, H-1'), 6.78 (m, 4H, 4×H-DMTr), 6.49 (d, 1H, *J* = 3.8 Hz, H-7), 4.66 (m, 1H, H-3'), 4.06 – 4.18 (m, 1H, H-4'), 3.75 (s, 3H, CH₃-DMTr-a), 3.75 (s, 3H, CH₃-DMTr-b), 3.38 (m, 2H, 2×H-5'), 2.65 (ddd, 1H, *J*_{gem} = 13.5, Hz, *J*₂ = 6.4 Hz, *J*₃ = 6.4 Hz, H-2'a), 2.48 (ddd, 1H, *J*_{gem} = 13.5 Hz, *J*_{2'b, 1'} = 6.1 Hz, *J*_{2'b, 3'} = 3.9 Hz, H-2'b)..

Deazapurin-9-yl)-5-(4,4-dimethoxytrityl)-1,2-dideoxy-D-ribofuranos-3-yl]-2-cyanoethyl-N,N-bis(isopropylamino)phosphoramidite. Established procedures were used for generation of the phosphoramidites and synthesis of the oligonucleotides on an Applied Biosystems 394 automatic DNA synthesizer (33,34). The phosphoramidite was obtained as a colorless oil, yield 40 %. MS (ESI, MeCN, LiCl added, neg.): 758 (M +35 [Cl]). MS (ESI, MeCN, LiCl added, neg.): 730 (M +7 [Li]). ³¹P NMR (400 MHz, MeCN-*d*3): 149.04 (s, 1.st diastereoisomer), 148.92 (s, 2.nd diastereoisomer).

Incorporation Assays with Pol α and BF—All kinetic data were determined under steady state conditions. Reactions (5 μL) typically contained 5 nM pol α or BF, 1 μM 5'-[³²P]-primer/template, 50 mM Tris-HCl pH 8.0, 1 mM dithiothreitol, 0.1 mg/mL bovine serum albumin, 10 mM MgCl₂, 5% glycerol, and various concentrations of a dNTP (analogue). Reactions were

incubated at 37°C for 5–30 min and quenched with 5 μ L formamide/0.05% xylene cyanol and bromophenol blue. Products were separated using 25% polyacrylamide, 8 M urea gels and imaged using a Typhoon Phosphorimager (Molecular Dynamics). Kinetic parameters were determined by fitting the data to the Michaelis-Menten equation using Origin 6.1 graphing software.

Binding Assays with Pol α and BF—The relative affinity of pol α and BF for modified DNAs was measured in assays containing 5 nM enzyme, 50 mM Tris-HCl pH 8.0, 1 mM dithiothreitol, 0.1 mg/mL bovine serum albumin, 10 mM MgCl₂, 5% glycerol, 1 μ M 5'-[³²P]-DNA_T, 5 μ M dATP, and various concentrations of DNA_G, DNA_I, or DNA_{OG}. Reactions were incubated at 37°C for 15 min and quenched with 5 μ L formamide/0.05% xylene cyanol and bromophenol blue. Products were separated using 25% polyacrylamide, 8 M urea gels and imaged using a Typhoon Phosphorimager (Molecular Dynamics). The amount of activity on DNA_T was quantified, and the relative ability of DNA_G, DNA_I, and DNA_{OG} to inhibit elongation of the 5'-[³²P]-DNA_T quantified.

Results

Both DNA pol α and BF generate 8-oxoG:A and I:A base-pairs much more rapidly than one might predict. Potentially, the relatively rapid formation of both base-pairs could result from Hoogsteen-type base-pairing between the purines (Figure 1). To better understand the mechanism by which pol α and BF generate these base-pairs, we used primer:templates of defined sequences (Figure 2) and nucleotide analogues modified at N1, N3, N⁶, and N7 (Figure 3).

Pol. α

We initially examined the effect of removing N7 from a purine dNTP on the correct incorporation of a dNTP (Table 1). Converting dATP into 7-deaza-dATP decreased the efficiency of polymerization opposite T by only around 3-fold, and converting purine dNTP into 7-deazapurine dNTP affected incorporation opposite T by 3.6-fold. Similarly, removing N7 from adenosine and purine in the template had only small effects (< 4-fold) on polymerization of dTTP across from the adenine analogues. The loss of N7 from adenine and purine also did not impact formation of incorrect G:A (analogue) mispairs. These data indicate that in both the incoming dNTP and the template base, N7 plays a relatively minor role during correct incorporation and preventing misincorporation opposite G.

Similar to previous data (20), pol α incorporated dATP opposite 8-oxoG more rapidly than it incorporated dCTP (Table 2). However, since the efficiency of dATP incorporation was no better than a natural mismatch, pol α clearly recognizes the A:8-oxoG base-pair as “wrong”. Most modifications further reduced polymerization, since removing N1, N⁶ or N7 from dATP resulted in no detectable incorporation.

Next, we examined how removing N3 from dATP and dGTP affected the efficiency with which pol α polymerized the resulting 3-deaza-dNTPs across from 8-oxoG. Previous work showed that removing N3 from dATP and dGTP greatly increases pol α -catalyzed misincorporation of the resulting 3-deazapurine dNTPs opposite some natural template bases (6), suggesting that this modification could affect incorporation opposite 8-oxoG. Remarkably, pol α incorporated 3-deaza-dATP 32-fold more efficiently than dATP across from 8-oxoG (Table 2). In contrast, pol α did not detectably incorporate 3-deaza-dGTP opposite 8-oxoG. Removing N⁶ from 3-deaza-dATP significantly inhibited polymerization of the resulting 3-deazapurine dNTP opposite 8-oxoG. Thus, N⁶ and N³ serve important and opposite functions during polymerization of dATP across from 8-oxoG.

In contrast to pol α incorporating dATP more efficiently than dCTP opposite 8-oxoG, the enzyme incorporated 8-oxo-dGTP more efficiently across from C than A (Table 2). In addition, pol α incorporated 8-oxo-dGTP opposite various adenine analogues much more efficiently than when it polymerized the corresponding analogue dNTPs opposite 8-oxoG in the template. Removing N7 from either adenine or purine had only small effects on 8-oxo-dGTP incorporation, while eliminating N⁶ from adenine had a slightly larger effect. Thus, neither N7 nor N⁶ appear critical for polymerization of 8-oxo-dGTP opposite A.

Pol α exhibited remarkably inconsistent interactions with the adenine analogues during generation of an adenine: hypoxanthine base-pair (Table 3). When the template contained the hypoxanthine, removing N⁶ from dATP inhibited incorporation by only 2-fold, while removing N⁶ from 7-deaza-dATP inhibited polymerization by >300-fold. N7 had similarly unpredictable effects – removing it from dATP increased incorporation, whereas removing it from purine dNTP severely inhibited incorporation across from hypoxanthine. Removing N3 from dATP increased incorporation opposite hypoxanthine by 7-fold, a much smaller effect than observed during incorporation opposite 8-oxoG. Effects of altering N⁶ and N7 in the template likewise had unpredictable effects on dITP incorporation. For example, when the template base contained N7, removing N⁶ only slightly inhibited dITP incorporation (~2-fold, compare dATP and purine dNTP, Table 3), but if the template base lacked N7, removing N⁶ increased polymerization by >10-fold (compare 7-deaza-dATP and 7-deazapurine dNTP).

To better understand the interactions of pol α with templates containing modified bases, we first determined if the identity of the next template base to be replicated affects DNA binding. Polymerase activity was monitored via dATP polymerization on DNA_T, and inhibition of polymerase activity by DNA_G, DNA_{OG}, and DNA_I measured. Since these DNAs only differ in the next template base to be replicated (Figure 2), comparing how well they inhibit pol α shows the effect of varying this base on binding. Importantly, DNA_{OG} and DNA_I inhibited dATP polymerization only 6.4- and 1.5-fold worse than DNA_G, indicating that the presence of these base analogues in the DNA did not greatly inhibit binding (Table 4). Then, we examined polymerization of a “low fidelity” dNTP opposite both 8-oxoG and hypoxanthine (Table 5). Pol α incorporates 6-nitrobenzimidazole dNTP opposite all 4 natural template bases much faster than an incorrect, natural dNTP (6). Likewise, pol α incorporated 6-nitrobenzimidazole dNTP opposite 8-oxoG, hypoxanthine, and G with similar efficiencies. In combination with the data showing rapid incorporation of 3-deaza-dATP, these results show that pol α can both productively bind templates containing 8-oxoG and also efficiently polymerize some dNTPs.

DNA Polymerase I from *B. stearothermophilus* (BF)

We extended these studies to BF, an A-family polymerase, by first examining the role of N7 during generation of A:T base pairs (Table 6). During incorporation of TTP opposite A, N7 plays a minor role since converting adenine into 7-deaza-adenine only decreased the efficiency of polymerization by 2.5-fold, and removing N7 from purine actually increased the incorporation efficiency by 7-fold. Removing N7 from dATP and purine dNTP reduced the polymerization efficiency opposite T by 11- and 3-fold, respectively, indicating that N7 has a slightly more significant impact in the dNTP. Removing N7 from either the incoming dNTP or the template base did not affect generation of incorrect A:G base pairs, indicating that N7 does not help prevent generation of A:G mispairs.

BF requires N⁶ for efficient polymerization of dATP opposite hypoxanthine as well as for polymerization of dITP opposite A (Table 7). Both with the template nucleotide and the triphosphate, removing N⁶ from either adenine or 7-deaza-adenine decreased formation of a base pair with hypoxanthine by >100-fold. Removing N7 from adenine also inhibited formation of a base pair with hypoxanthine, albeit to a lesser extent. Removing N7 from dATP inhibited

polymerization opposite hypoxanthine by just 3-fold, while removing N7 from a template A reduced incorporation of dITP by 18-fold. Eliminating N1 from dATP had little effect on the efficiency of incorporation of the resulting 1-deaza-dATP.

Unlike pol α , BF readily incorporates 8-oxo-dGTP opposite A (Table 8). Indeed, the efficiency of this polymerization event approaches that for a correct, canonical base pair. Removing N⁶ from the template A reduced 8-oxo-dGTP polymerization 85-fold, while removing N7 reduced incorporation by 9-fold. The further loss of N⁶ from 7-deaza-adenine reduced the efficiency of 8-oxo-dGTP polymerization by another 9-fold such that BF polymerizes 8-oxo-dGTP opposite both purine and 7-deazapurine with similar efficiencies. When BF polymerizes dATP opposite 8-oxoG, the loss of either N7 or N⁶ from dATP reduces incorporation to undetectable levels. We also explored the effect of removing N1 since it could be involved in hydrogen bonding to 8-oxoG. BF polymerized 1-deaza-dATP 17-fold less efficiently than dATP opposite 8-oxoG. Thus, N1, N⁶ and N7 all appear important for efficient polymerization of dATP opposite 8-oxoG.

To better understand how BF interacts with templates containing an 8-oxoG or hypoxanthine lesion, we tested the ability of BF to incorporate 6-trifluorobenzimidazole dNTP, a relatively low fidelity dNTP (28), opposite 8-oxoG, hypoxanthine, and G (Table 5). While BF incorporated 6-trifluorobenzimidazole dNTP opposite hypoxanthine only 2-fold less well than it incorporated dATP, incorporation opposite 8-oxoG was no better than incorporation of dATP or dCTP. The effects of varying the template base to be replicated on DNA binding was measured by comparing the ability of DNA_G, DNA_{OG}, and DNA_I to inhibit BF activity on a separate template. Replacing the template G with hypoxanthine reduced binding by 1.2-fold, while replacing G with 8-oxoG reduced binding by 6.3-fold (Table 4).

Discussion

The interactions of an A-family polymerase, BF, and a B-family polymerase, pol α , with two base lesions were examined using a series of purine analogues modified at N1, N3, N⁶ and N7. The two enzymes showed distinctly different requirements for generating base pairs involving either hypoxanthine or 8-oxoG, consistent with previous studies showing that polymerases from different families have discrete mechanistic constraints.

Pol α discriminated strongly against polymerization of any natural dNTP opposite the 8-oxoG lesion. Consistent with previous studies (27), the enzyme incorporated dATP most efficiently. Loss of N1, N⁶, or N7 reduced polymerization to undetectable levels, as did conversion to another natural base (Table 2). However, removing N3 increased incorporation 32-fold, indicating that N3 acts as a critical “gatekeeper” to prevent incorporation of dATP opposite 8-oxoG. Analogously, we previously found that removing N3 from dATP and dGTP markedly increased some misincorporation events (6). These data suggest that pol α may use the chemical features of N3 to prevent many, but certainly not all, incorrect purine dNTP polymerization reactions. How N3 has this effect remains unclear, although as noted previously, we suspect that it involves an interaction with Tyr 957 (6). Interestingly, pol α did not efficiently polymerize 3-deaza-dGTP opposite 8-oxoG, indicating that the other functional groups on guanine are sufficient to prevent this polymerization event.

Removing N⁶ from 3-deaza-dATP resulted in no detectable incorporation of the resulting 3-deazapurine dNTP across from 8-oxoG. Since N⁶ forms a hydrogen bond in a Hoogsteen base pair between 3-deaza-adenine and 8-oxoG (Figure 1B), this large decrease in incorporation suggests that pol α incorporates 3-deaza-dATP via a Hoogsteen base pair. This base pair could be either 8-oxoG (*syn*): A (*anti*) or 8-oxoG (*anti*): A (*syn*), because N⁶ forms a hydrogen bond in both potential Hoogsteen base pairs (Figure 1B). Deleting N⁶ from dATP also decreased

incorporation of the resulting purine NTP opposite 8-oxoG, again consistent with formation of a Hoogsteen base pair. However, these latter data must be interpreted more cautiously due to the low efficiency of dATP.

Pol α also can incorporate dNTPs opposite 8-oxoG without forming any hydrogen bonds since radically modifying the base to 6-nitrobenzimidazole resulted in a dNTP that pol α very efficiently incorporated (Table 5). Thus, the pol α active site has evolved to prevent incorporation of natural dNTPs opposite 8-oxoG, but not unnatural dNTPs that lack specific chemical features of a natural base. Indeed, pol α employs this type of negative selectivity to prevent misincorporation of natural dNTPs opposite a natural base (6).

In contrast to the strong discrimination against polymerizing natural dNTPs across from 8-oxoG in the template, pol α polymerized 8-oxo-dGTP relatively efficiently against C, and about 10-fold less efficiently opposite A. The more efficient polymerization opposite C suggests that in the pol α active site, 8-oxo-dGTP binds in the *anti* conformation, since it is difficult to see how binding in the *syn* conformation would result in efficient incorporation. Indeed, the ca. 100-fold less efficient polymerization of 8-oxo-dGTP opposite C as compared to dGTP opposite C could result from the reduced stability of the *anti* conformation as compared to the *syn* conformation.

N⁶ of a template A enhances the polymerization of 8-oxo-dGTP, while N7 plays little if any role. These data are consistent with two models for how pol α binds and polymerizes 8-oxo-dGTP across from a template A – 8-oxo-dGTP binds in the *anti* conformation and forms a larger than normal Watson-Crick type base-pair, or 8-oxo-dGTP binds in the *syn* conformation and forms a Hoogsteen base-pair with the A. Given the greater stability of the *syn* conformation and that structural studies of double-stranded DNA show 8-oxoG and A form a Hoogsteen base-pair (13,14), this is currently our favored model.

Removing N² from either dGTP or a template G stimulates the formation of incorrect A: hypoxanthine base pairs (27). During polymerization of dTTP, removing N7 from both adenine and purine in the template inhibited polymerization (by >100- and 4-fold, respectively). In contrast, losing N⁶ from a template A slightly decreased dTTP polymerization, whereas losing N⁶ from 7-deaza-adenine greatly stimulated polymerization. While the decreased polymerization in the absence of N7 is consistent with a Hoogsteen type base-pair between adenine and hypoxanthine, the effects of deleting N⁶ are not (Figure 1A). Thus, if a Hoogsteen base-pair is formed in this case, the putative hydrogen bond between N⁶ of adenine and O⁶ of hypoxanthine is energetically irrelevant. Alternatively, and as described in greater detail below, these data are consistent with the hypothesis that the identity of the template base being replicated alters how pol α identifies the “correct” incoming dNTP. As with incorporation opposite 8-oxoG, pol α very efficiently incorporated the low fidelity base 6-nitrobenzimidazole dNTP, again indicating the key role that negative selectivity can play in preventing incorporation of incorrect natural dNTPs.

Modifications to the template base had inconclusive effects on dNTP polymerization by pol α . For example, removing N⁶ from adenine inhibits polymerization of dTTP, whereas removing N⁶ from 7-deazaadenine had no effect on polymerization (Table 1). Analogously, removing N⁶ from a template adenine slightly inhibited polymerization of dTTP (2-fold, Table 3)), but removing N⁶ from 7-deazaadenine greatly enhanced dTTP polymerization. These very different effects of the same base modification indicate that the extent to which the interactions between pol α and a specific functional group enhance (or prevent) dNTP incorporation depends upon the overall structure of the base. Additionally, they indicate that the properties of the template base alone can help determine what dNTP(s) pol α will efficiently polymerize. In this model,

pol α “reads” the template base and depending upon the structure of the base, slightly alter its conformation to optimize its ability to choose the correct dNTP.

Interestingly, three lines of evidence indicate that the A family polymerases also “read” the template base in order to enhance selection of the correct dNTP. Similar to pol α , the identical base modification in two different template bases can have very different effects on both BF and Klenow Fragment (8,28). Waksman and coworkers showed that both the structure of the closed E-DNA-dNTP ternary complexes vary depending upon the identity of the template base (35). Finally, the dynamics of dNTP polymerization also vary according to the identity of the template base (36). Thus, the template base itself, as opposed to just the properties of the base-pair formed between the incoming dNTP and template base, can greatly affect how DNA polymerases differentiate “right” from “wrong” dNTPs.

BF requires both N⁶ and N7 of a template adenine for efficient polymerization of dITP, suggesting that misincorporation of dITP involves a Hoogsteen base-pair. During polymerization of dATP opposite a template hypoxanthine, BF again requires N⁶ for efficient polymerization. Curiously, however, removal of either N1 or N7 also inhibited incorporation, albeit to a lesser extent than removing N⁶. While the effects of removing N7 suggest formation of a Hoogsteen base-pair, the effects of losing N1 are not consistent with this model. Resolving this question will likely require capturing a catalytically relevant structure of BF during polymerization of dATP opposite hypoxanthine.

BF polymerized 8-oxo-dGTP opposite a template A remarkably efficiently – much more efficiently than opposite C and with similar efficiency as a correct dNTP. N⁶ clearly plays an important role in this process since removing it from either adenine or 7-deaza-adenine inhibited polymerization. Removing N7 from a template adenine decreased incorporation less than removing N⁶, while removing N7 from purine had no effect. This modification also modestly affected correct incorporation of dTTP. Why removing N7 has these effects remains unclear. Structural studies of BF and KlenTaq, another A family polymerase, do not reveal any obvious interactions of N7 with the protein (37). Rather, these effects may reflect subtle changes in the electron distribution around the base that BF can detect, or they could reflect interactions prior to formation of the closed E-DNA-dNTP complex.

Similar to pol α , BF discriminated much more strongly against incorporating dATP opposite a template 8-oxoG than it did against incorporating 8-oxo-dGTP opposite A (70-fold). Additionally, the enzyme was very sensitive to removing N1, N⁶, or N7, again similar to pol α . While the effects of removing N1 and N⁶ are consistent with Hoogsteen base pairing between 8-oxoG and A, the effects of removing N7 are difficult to rationalize in terms of the structure of a base-pair.

The potential mutagenicity of 8-oxo-dGTP and 8-oxoG in the template heavily depends upon the polymerase with which they interact. Unfortunately, one cannot predict the incorporation frequency even among polymerases in the same family. Among A family enzymes, BF incorporates 8-oxo-dGTP extremely well opposite A, while other members of this family have very different efficiencies. For example, pol γ incorporates 8-oxo-dGTP opposite A 250-fold less efficiently than dGTP opposite C (38), while pol I (*E. coli*) polymerizes 8-oxo-dGTP extremely poorly (4). Similarly, different A family polymerases exhibit very different capacities to replicate past an 8-oxoG template lesion. Perhaps more surprising, the relative efficiency of generating C:8-oxoG versus A:8-oxoG base pairs varies by at least 70-fold among A family enzymes (39). These data indicate that different A family active sites interact extremely differently with 8-oxoG.

Likewise, the B family polymerases show large variability in terms of polymerization efficiency of 8-oxo-dGTP, replication past a template 8-oxoG lesion, and the ratio of A:8-oxoG

versus C:8-oxoG base pair formation efficiency (4,20–22). As with the A family enzymes, these data indicate that one cannot stereotype how the B family enzymes will interact. One of the most biologically curious disparities is how pol α and pol δ interact with 8-oxoG in the template (20). Pol α does not efficiently bypass it, but pol δ does, even though both enzymes are replicative polymerases. This dichotomy is particularly perplexing based on recent data indicating that the primary role of both enzymes is Okazaki fragment synthesis (40). Why biology allowed these two enzymes to process the same lesion so differently, and what causes these two active sites to have such different properties, remains unclear.

References

1. Kunkel TA, Bebenek K. Recent Studies on the Fidelity of DNA Synthesis. *Biochim. Biophys. Acta* 1988;951:1–15. [PubMed: 2847793]
2. Patro JN, Wiederholt CJ, Jiang YL, Delaney JC, Essigmann JM, Greenberg MM. Studies on the Replication of the Ring-Opened Formamidopyrimidines, Fapy dG in *E. coli*. *Biochemistry* 2007;46:10202–10212. [PubMed: 17691820]
3. Imoto S, Patro JN, Jiang YL, Greenberg MM. Synthesis, DNA Polymerase Incorporation, and Enzymatic Phosphate Hydrolysis of Formamidopyrimidine Nucleoside Triphosphates. *J. Am. Chem. Soc* 2006;128:14606–14611. [PubMed: 17090045]
4. Einolf HJ, Schnetz-Boutaud N, Guengerich FP. Steady-State and Pre-Steady-State Kinetic Analysis of 8-Oxo-7,8-dihydroguanosine Triphosphate Incorporation and Extension by Replicative and Repair DNA Polymerases. *Biochemistry* 1998;37:13300–13312. [PubMed: 9748338]
5. Lowe LG, Guengerich FP. Steady-State and Pre-Steady State Kinetic Analysis of dNTP Insertion Opposite 8-Oxo-7,8-dihydroguanine by *Escherichia coli* Polymerase I exo^- and II exo^- . *Biochemistry* 1996;35:9840–9849. [PubMed: 8703958]
6. Beckman J, Kincaid K, Hocek M, Spratt T, Engels J, Cosstick R, Kuchta RD. Human DNA Polymerase α Uses a Combination of Positive and negative Selectivity to Polymerize Purine dNTPs with High Fidelity. *Biochemistry* 2007;46:448–460. [PubMed: 17209555]
7. Sintim HO, Kool ET. Remarkable Sensitivity to DNA Base Shape in the DNA Polymerase Active Site. *Angew. Chem. Int. Ed* 2006;45:1974–1979.
8. Kincaid K, Beckman J, Zivkovic A, Halcomb RL, Engels JW, Kuchta RD. Exploration of Factors Driving Incorporation of Unnatural dNTPs into DNA by Klenow Fragment (DNA Polymerase I) and DNA Polymerase α . *Nucleic Acids Res* 2005;33:2620–2628. [PubMed: 15879351]
9. Chiramonte M, Moore CL, Kincaid K, Kuchta RD. Facile Polymerization of dNTPs Bearing Unnatural Base Analogues by DNA Polymerase α and Klenow Fragment (DNA Polymerase I). *Biochemistry* 2003;42:10472–10481. [PubMed: 12950174]
10. Steenken S, Jovanovic SV. How Easily Oxidizable is DNA? One-Electron Reduction Potentials of Adenosine and Guanosine Radicals in Aqueous Solution. *J. Am. Chem. Soc* 1997;119:617–618.
11. Wang D, Kreutzer DA, Essigmann JM. Mutagenicity and repair of oxidative DNA damage: insights from studies using defined lesions. *Mutat. Res* 1998;400:99–115. [PubMed: 9685598]
12. Nakabeppu Y, Sakumi K, Sakamoto K, Tsuchimoto D, Tsuzuki T, Nakatsu Y. Mutagenesis and carcinogenesis caused by the oxidation of nucleic acids. *Biol. Chem* 2006;387:373–379. [PubMed: 16606334]
13. Kouchakdjian M, Bodepudi V, Shibutani S, Eisenberg M, Johnson F, Grollman AP, Patel DJ. NMR structural studies of the ionizing radiation adduct 7-hydro-8-oxodeoxyguanosine (8-oxo-7H-dG) opposite deoxyadenosine in a DNA duplex. 8-Oxo-7H-dG(syn)•dA(anti) alignment at lesion site. *Biochemistry* 1991;30:1403–1412. [PubMed: 1991121]
14. Lipscomb LA, Peek ME, Morningstar ML, Verghis SM, Miller EM, Rich A, Essigmann JM, Williams LD. X-ray structure of a DNA decamer containing 7,8-dihydro-8-oxoguanine. *Proc. Natl. Acad. Sci. USA* 1995;92:719–723. [PubMed: 7846041]
15. Henderson PT, Delaney JC, Gu F, Tannenbaum SR, Essigmann JM. Oxidation of 7,8-Dihydro-8-oxoguanine Affords Lesions That Are Potent Sources of Replication Errors in Vivo. *Biochemistry* 2002;41:914–921. [PubMed: 11790114]

16. Cheng KC, Cahill DS, Kasai H, Nishimura S, Loeb L. 8-Hydroxyguanine, an Abundant Form of Oxidative DNA Damage, Causes G→T and A→C Substitutions. *J. Biol. Chem* 1992;267:166–172. [PubMed: 1730583]
17. Tassotto ML, Mathews CK. Assessing the Metabolic Function of the Mut T 8-Oxodeoxyguanosine Triphosphatase in *Escherichia coli* by Nucleotide Pool Analysis. *J. Biol. Chem* 2002;277:15807–15812. [PubMed: 11856756]
18. Wilson DM, Bohr VA. The mechanics of base excision repair, and its relationship to aging and disease. *DNA Repair* 2007;6:544–559. [PubMed: 17112792]
19. Kuznetsova SA, Rykhlevskaya AI. Mono- and Bifunctional DNA Glycosylases Involved in Repairing Oxidatively Damaged DNA. *Molecular Biology* 2000;34:860–874.
20. Shibutani S, Takeshita M, Grollman AP. Insertion of Specific Bases During DNA Synthesis Past the Oxidative-Damaged Base 8-Oxo dG. *Nature* 1991;349:431–432. [PubMed: 1992344]
21. de Vega M, Salas M. A highly conserved Tyrosine residue of family B DNA polymerase contributes to dictate translesion synthesis past 8-oxo-7,8-dihydro-2'-deoxyguanosine. *Nucleic Acids Res* 2007;35:5096–5107. [PubMed: 17652324]
22. Freisinger E, Grollman AP, Miller H, Kisker C. Lesion (in)tolerance reveals insights into DNA replication fidelity. *EMBO* 2004;23:1494–1505.
23. Leonard GA, Guy A, Brown T, Teoule R, Hunter WN. Conformation of Guanine-8-Oxoadenine Base Pairs in the Crystal Structure of d(CGCGAATT(O8A)GCG). *Biochemistry* 1992;31:8415–8420. [PubMed: 1390625]
24. McAuley-Hecht KE, Leonard GA, Gibson NJ, Thomson JB, Watson WP, Hunter WN, Brown T. Crystal Structure of a DNA Duplex Containing 8-Hydroxydeoxyguanine-Adenine Base Pairs. *Biochemistry* 1994;33:10266–10270. [PubMed: 8068665]
25. Hsu GW, Ober M, Carell T, Beese LS. Error-prone replication of oxidatively damaged DNA by a high-fidelity DNA polymerase. *Nature* 2004;431:217–221. [PubMed: 15322558]
26. Broyde S, Wang L, Rechko O, Geacintov NE, Patel DJ. Lesion processing: high-fidelity versus lesion-bypass DNA polymerases. *TIBS* 2008;33:209–219. [PubMed: 18407502]
27. Patro JN, Urban M, Kuchta RD. Role of the 2-Amino Group of Purines during dNTP Polymerization by Human DNA Polymerase α . *Biochemistry* 2009;48:180–189. [PubMed: 19072331]
28. Trostler M, Delier A, Beckman J, Urban M, Patro JN, Spratt TE, Beese LS, Kuchta RD. Discrimination between Right and Wrong Purine dNTPs by DNA Polymerase I from *Bacillus stearothermophilus*. *Biochemistry*. 2009In Press
29. Zerbe LK, Goodman MF, Efrati E, Kuchta RD. Abasic Template Lesions are Strong Chain Terminators for DNA Primase but not for DNA Polymerase Alpha During Synthesis of new DNA Strands. *Biochemistry* 1999;38:12908–12914. [PubMed: 10504262]
30. Cavanaugh N, Kuchta RD. Initiation of New DNA Strands by the Herpes Simplex Virus-1 Primase-Helicase Complex and Either Herpes DNA Polymerase or Human DNA Polymerase. *J. Biol. Chem* 2009;284:1523–1532. [PubMed: 19028696]
31. Kuchta RD, Mizrahi V, Benkovic PA, Johnson KA, Benkovic SJ. Kinetic Mechanism of DNA Polymerase I (Klenow). *Biochemistry* 1989;26:8410–8417. [PubMed: 3327522]
32. Sambrook, J.; Fritsch, EF.; Maniatis, T. *Molecular Cloning: A Laboratory Manual*. Cold Spring Harbor, NY: Cold Spring Harbor Laboratories; 1989.
33. Beaucage SL, Caruthers MH. Deoxynucleoside Phosphoramidites- A New Class of Key Intermediates for Deoxypolynucleotide Synthesis. *Tet. Lett* 1981;22:1859–1862.
34. McBride LJ, Caruthers MH. An Investigation of Several Deoxynucleoside Phosphoramidites Useful for Synthesizing Deoxynucleotides. *Tet. Lett* 1983;24:245–248.
35. Li Y, Kong Y, Korolev S, Waksman G. Crystal structures of the Klenow fragment of *Thermus aquaticus* DNA polymerase I complexed with deoxyribonucleoside triphosphates. *Protein Sci* 1998;7:1116–1123. [PubMed: 9605316]
36. Rothwell PJ, Waksman G. A Pre-equilibrium before Nucleotide Binding Limits Fingers Subdomain Closure by Klenow. *J. Biol. Chem* 2007;282:28884–28892. [PubMed: 17640877]
37. Kim Y, Eom SH, Wang J, Lee D-S, Suh SW, Steitz TA. Crystal structure of *Thermus aquaticus* DNA polymerase. *Nature* 1995;376:612–616. [PubMed: 7637814]

38. Hanes JW, Thai DM, Johnson KA. Incorporation and Replication of 8-Oxo-deoxyguanosine by the Human Mitochondrial DNA Polymerase. *J. Biol. Chem* 2006;281:36241–36248. [PubMed: 17005553]
39. Brown JA, Duym WW, Flower JD, Zucal S. Single-turnover Kinetic Analysis of the Mutagenic Potential of 8-Oxo-7,8-dihydro-2'-deoxyguanosine during Gap-filling Synthesis Catalyzed by Human DNA Polymerases λ and β . *J. Mol. Biol* 2007;367:1258–1269. [PubMed: 17321545]
40. Pavlov YI, Frahm C, McElhinny SAN, Niimi A, Suzuki M, Kunkel TA. Evidence the Errors Made by DNA Polymerase α are Corrected by DNA Polymerase δ . *Current Biology* 2006;16:202–207. [PubMed: 16431373]

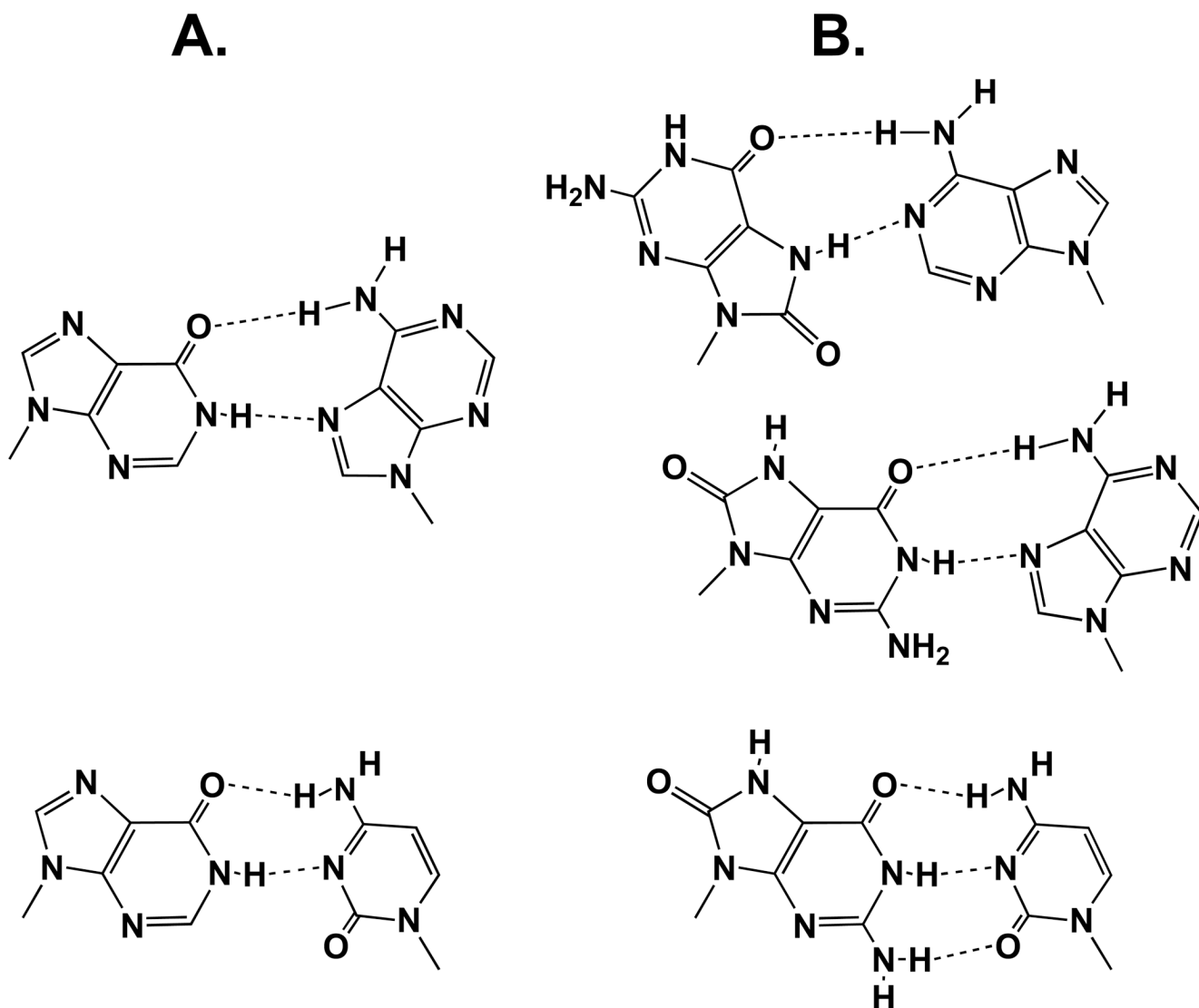


Figure 1. Hydrogen bonding schemes of (A) hypoxanthine base paired with A in the *anti* and *syn* conformations, respectively, and base paired with C, and (B) 8-oxoG in the *syn* and *anti* conformation base paired with A in the *anti* and *syn* conformations, respectively, and 8-oxoG in the *anti* conformation base paired with C.

DNA _A	5'- TCC ATA TCA CAT 3'- AGG TAT AGT GTA ATT CTT ATC ATC T
DNA _C	5'- TCC ATA TCA CAT 3'- AGG TAT AGT GTA CTT CTT ATC ATC T
DNA _G	5'- TCC ATA TCA CAT 3'- AGG TAT AGT GTA GAT CTT ATC ATC T
DNA _T	5'- TCC ATA TCA CAT 3'- AGG TAT AGT GTA TAT CTT ATC ATC T
DNA _I	5'- TCC ATA TCA CAT 3'- AGG TAT AGT GTA ICT CTT ATC ATC T
DNA _{OG}	5'- TCC ATA TCA CAT 3'- AGG TAT AGT GTA (OG) CT CTT ATC ATC T

Figure 2.
Primer-templates used. I = hypoxanthine and OG = 8-oxoG. The letter(s) after 'DNA' identifies the next template base to be replicated.

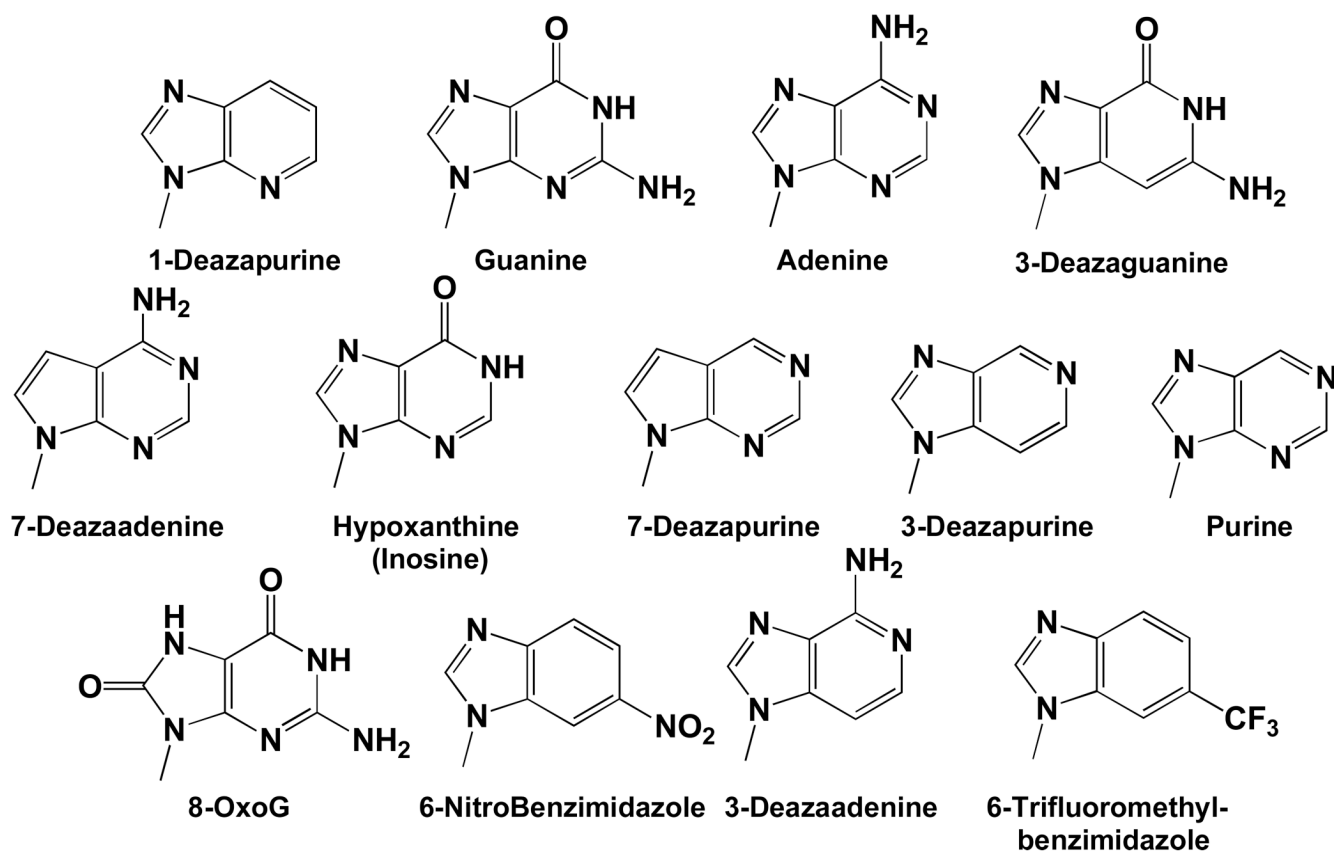


Figure 3.
Bases used in these studies.

Table 1Incorporation of natural and analogue dNTPs by pol α opposite both natural and analogue template nucleosides.

dNTP	Template Base	k_{cat} (min^{-1})	K_M (μM)	k_{cat}/K_M ($\mu\text{M}^{-1}\text{min}^{-1}$)
dCTP	G	18.4 ± 1.8	2.6 ± 0.4	7.0
dTTP	A	17.8 ± 1.0	6.0 ± 1.3	3.0
	P	9.6 ± 0.2	5.5 ± 0.9	1.7
	7DA	3.4 ± 0.2	4.4 ± 2	0.77
	7DP	5.2 ± 0.2	7.1 ± 1.7	0.73
dGTP	A			N/A ^a
	P			N/A
	7DA			N/A
	7DP			N/A
	C	24.4 ± 0.8	3.3 ± 0.6	7.4
dATP	T	8.6 ± 0.9	1.2 ± 0.3	7.2
	G	0.36 ± 0.008	1330 ± 280	2.7×10^{-4}
dPTP	T	3.8 ± 0.2	1.3 ± 0.4	2.9
7DdATP	T	5.4 ± 0.4	2.0 ± 0.8	2.7
	G			N/A
7DdPTP	T	2.8 ± 0.2	3.6 ± 1.1	0.78
	G			N/A
1DdATP	G	1.7 ± 0.2	700 ± 190	2.4×10^{-3}
3DdATP	T	19.6 ± 0.4	2.8 ± 0.2	7.0
	G	0.5 ± 0.02	730 ± 65	7.1×10^{-4}

^aN/A Incorporation was too low to measure accurately.

Table 2

Incorporation of dNTPs by pol α opposite 8-oxoG and incorporation of 8-oxo-dGTP opposite both natural and analogue template nucleosides.

dNTP	Template	k_{cat} (min^{-1})	K_M (μM)	k_{cat}/K_M ($\mu\text{M}^{-1} \text{min}^{-1}$)
8-Oxo-dGTP	A	1.9 ± 0.1	840 ± 120	2.2×10^{-3}
	P	0.20 ± 0.04	930 ± 360	2.2×10^{-4}
	7DA	1.0 ± 0.01	1100 ± 260	9.1×10^{-4}
	7DP	0.10 ± 0.02	210 ± 110	4.8×10^{-4}
	C	4.4 ± 1.0	290 ± 110	1.5×10^{-2}
dATP	8-OxoG	0.08 ± 0.004	400 ± 90	2.0×10^{-4}
3DdATP	8-OxoG	0.1 ± 0.08	16 ± 5	6.3×10^{-3}
3DdPTP	8-OxoG			N/A ^a
dPTP	8-OxoG			N/A
7DdATP	8-OxoG			N/A
1DdATP	8-OxoG			N/A
7DdPTP	8-OxoG			N/A
3DdGTP	8-OxoG			N/A
dCTP	8-OxoG			N/A

^aN/A Incorporation was too low to measure accurately.

Table 3

Polymerization of dITP opposite natural and analogue template nucleosides and polymerization of natural and analogue dNTPs opposite a template hypoxanthine by pol α .

dNTP	Template	k_{cat} (min^{-1})	K_M (μM)	k_{cat}/K_M ($\mu\text{M}^{-1}\text{min}^{-1}$)
dITP	A	3.2 ± 0.4	320 ± 100	1.0×10^{-2}
	P	0.8 ± 0.1	180 ± 50	4.4×10^{-3}
	7DA			N/A ^a
	7DP	0.60 ± 0.08	480 ± 180	1.1×10^{-3}
	3DA	0.32 ± 0.05	830 ± 260	3.9×10^{-4}
	C	3.4 ± 0.1	2.1 ± 0.3	1.6
dATP	I	1.4 ± 0.4	230 ± 150	6.1×10^{-3}
dPTP	I	1.0 ± 0.1	260 ± 130	3.8×10^{-3}
7DdATP	I	3.2 ± 0.6	120 ± 50	2.7×10^{-2}
1DdATP	I	2.0 ± 0.2	990 ± 160	2.0×10^{-3}
3DdATP	I	7.8 ± 0.2	190 ± 20	4.1×10^{-2}
7DdPTP	I			N/A
dCTP	I	1.6 ± 0.08	1.6 ± 0.5	1.0

^aN/A Incorporation was too low to measure accurately.

Table 4IC₅₀ values for inhibition of pol α and BF by natural and modified DNAs.

DNA	Pol α	BF
	IC ₅₀ (nM)	IC ₅₀ (nM)
dG	85 \pm 40	460 \pm 70
dI	130 \pm 60	580 \pm 190
8-OxoG	550 \pm 300	2900 \pm 390

Table 5
Incorporation of “low fidelity” dNTPs by BF and pol α .

dNTP	Template	k_{cat} (min^{-1})	K_M (μM)	k_{cat}/K_M ($\mu\text{M}^{-1} \text{min}^{-1}$)
Pol α				
6NO2dBTP	G	6.4 ± 1.0	25 ± 11	0.25
	I	4.8 ± 0.2	15 ± 3	0.32
	8-OxoG	1.8 ± 0.2	7.0 ± 4.0	0.25
BF				
6CF3dBTP	G	20 ± 0.3	43 ± 2	0.46
	I	23 ± 3	90 ± 20	0.25
	8-OxoG	4.0 ± 0.4	130 ± 60	0.30

Table 6

Incorporation of natural nucleotides and analogues by BF across from both natural and analogue template nucleosides.

dNTP	Template	V_{\max} (%/min ⁻¹)	K_M (μM)	k_{cat}/K_M ($\mu\text{M}^{-1}\text{min}^{-1}$)
dCTP	G	19 ± 6.0	1.8 ± 0.5	10.4
dTTP	A	21 ± 2	8.2 ± 6	2.6
	P	62 ± 8	330 ± 90	0.19
	7DA	38 ± 8	38 ± 15	1.0
	7DP	8.4 ± 0.1	6.4 ± 0.4	1.3
dGTP	A	1.1 ± 0.4	390 ± 300	2.9×10^{-3}
	P			N/A ^a
	7DA			N/A
	7DP			N/A
	C	24 ± 2	19 ± 6	1.3
dATP	T	12.1 ± 0.6	2.2 ± 0.5	5.5
dPTP	T	4.4 ± 0.2	6.7 ± 1	0.66
7DdATP	T	21 ± 1	56 ± 10	0.37
	G			N/A
7DdPTP	T	36 ± 4	160 ± 40	0.23
	G			N/A
1DdATP	G	1.7 ± 0.2	340 ± 70	5.0×10^{-3}

^aN/A Incorporation was too low to accurately measure.

Table 7

Incorporation of dNTPs opposite a templating hypoxanthine and dITP opposite various templating nucleosides by BF.

dNTP	Template	V_{\max} (%/min ⁻¹)	K_M (μ M)	k_{cat}/K_M ($\mu\text{M}^{-1}\text{min}^{-1}$)
dITP	A	3.1 \pm 0.2	19 \pm 4.4	0.16
	P			N/A ^a
	7DA	2.3 \pm 0.2	260 \pm 80	8.8 $\times 10^{-3}$
	7DP			N/A
	C	55 \pm 4.0	79 \pm 24	0.69
dATP	I	5.3 \pm 0.4	130 \pm 40	4.0 $\times 10^{-2}$
dPTP	I			N/A
7DdATP	I	4.8 \pm 1	390 \pm 170	1.2 $\times 10^{-2}$
7DdPTP	I			N/A
1DdATP	I	25 \pm 1	480 \pm 50	5.3 $\times 10^{-2}$
dCTP	I	16 \pm 0.4	3.5 \pm 0.5	4.7

^aN/A Incorporation was too low to accurately measure.

Table 8

Incorporation of dNTPs opposite a template 8-oxoG and incorporation of 8-oxo dGTP opposite natural and analogue template nucleosides by BF.

dNTP	Template	V_{\max} (%/min ⁻¹)	K_M (μM)	k_{cat}/K_M ($\mu\text{M}^{-1}\text{min}^{-1}$)
8-Oxo-dGTP	A	33 ± 1	12 ± 2	2.8
	P	5.5 ± 0.6	165 ± 60	3.3 × 10 ⁻²
	7DA	5.6 ± 0.3	18 ± 5	0.31
	7DP	2.2 ± 0.2	70 ± 20	3.3 × 10 ⁻²
	C	11.5 ± 0.4	52 ± 6	0.22
dATP	8-OxoG	7.4 ± 0.6	190 ± 60	4 × 10 ⁻²
dPTP	8-OxoG			N/A ^a
7DdATP	8-OxoG			N/A
7DdPTP	8-OxoG			N/A
1DdATP	8-OxoG	1.3 ± 0.4	540 ± 20	2.4 × 10 ⁻³
dCTP	8-OxoG	29 ± 4	2000 ± 470	1.5 × 10 ⁻²

^aN/A Incorporation was too low to accurately measure.